

---

EFDA–JET–CP(03)01-28

S. Jachmich, Ph. Andrew, Y. Corre, P. Dumortier, T. Eich, A. Huber, A. Kallenbach,  
M. Laux, A. Loarte, G. Maddison, G. Matthews, A. Messiaen, P. Monier-Garbet,  
M. F. F. Nave, J. Ongena, R. Pitts, J. Strachan, RI-Mode Group  
and JET EFDA Contributors

# Study of Edge Properties and Power Deposition Profiles in JET ELMy H-Mode Discharges using Divertor Target Langmuir Probes



# Study of Edge Properties and Power Deposition Profiles in JET ELMy H-Mode Discharges using Divertor Target Langmuir Probes

S. Jachmich<sup>1</sup>, Ph. Andrew<sup>2</sup>, Y. Corre<sup>3</sup>, P. Dumortier<sup>1</sup>, T. Eich<sup>4</sup>, A. Huber<sup>5</sup>,  
A. Kallenbach<sup>4</sup>, M. Laux<sup>6</sup>, A. Loarte<sup>7</sup>, G. Maddison<sup>2</sup>, G. Matthews<sup>2</sup>, A. Messiaen<sup>1</sup>,  
P. Monier-Garbet<sup>8</sup>, M.F.F. Nave<sup>9</sup>, J. Ongena<sup>1</sup>, R. Pitts<sup>10</sup>, J. Strachan<sup>2</sup>,  
RI-Mode Group and JET EFDA Contributors\*

<sup>1</sup>Laboratory for Plasmaphysics, Ecole Royale Militaire/Koninklijke Militaire School, EURATOM-Association "Belgian State", Brussels, Belgium, Partners in the Trilateral Euregio Cluster (TEC)

<sup>2</sup>EURATOM/UKAEA Fusion Association, Culham Science Centre, Abingdon, OX14 3DB, UK

<sup>3</sup>KTH, Royal Institute of Technology, Association "EURATOM-VR", Stockholm, Sweden

<sup>4</sup>Max-Planck Institut fuer Plasmaphysik, Euratom Association, Garching, Germany

<sup>5</sup>Institut für Plasmaphysik, Forschungszentrum Jülich, Germany, Trilateral Euregio Cluster (TEC)

<sup>6</sup>Max-Planck-Institut für Plasmaphysik, Association EURATOM, Berlin, Germany

<sup>7</sup>EFDA Close Support Unit (Garching), Boltzmannstr. 2, Garching, Germany

<sup>8</sup>CEA Cadarache, France

<sup>9</sup>Associacao EURATOM/IST, Instituto Superior Tecnico, Lisbon, Portugal

<sup>10</sup>Centre Recherches Phys. Plasma, Association EURATOM-Switzerland, EPFL, Lausanne, Switzerland

\*See Annex of J. Pamela et al., "Overview of Recent JET Results and Future Perspectives", Fusion Energy 2000 (Proc. 18th Int. Conf. Sorrento, 2000), IAEA, Vienna (2001).

Preprint of Paper to be submitted for publication in Proceedings of the  
EPS Conference on Controlled Fusion and Plasma Physics,  
(St. Petersburg, Russia, 7-11 July 2003)

“This document is intended for publication in the open literature. It is made available on the understanding that it may not be further circulated and extracts or references may not be published prior to publication of the original when applicable, or without the consent of the Publications Officer, EFDA, Culham Science Centre, Abingdon, Oxon, OX14 3DB, UK.”

“Enquiries about Copyright and reproduction should be addressed to the Publications Officer, EFDA, Culham Science Centre, Abingdon, Oxon, OX14 3DB, UK.”

## ABSTRACT.

ELMy H-mode is the foreseen operational scenario for ITER. However the good confinement properties and high densities in this scenario are accompanied by the appearance of Type I ELMs which could possibly severely impact the lifetime of divertor and first wall components. Although Edge Localised Modes (ELMs) are a well-known phenomenon since the discovery of the H-mode, further improvements in diagnosis and modelling are still needed for a better understanding of ELM effects on wall elements in a tokamak. Langmuir probes embedded in the divertor are ideal for resolving local effects of ELMs on the divertor tiles. Using various techniques, such as triple probe operation, strike point sweeps and coherent averaging, spatial and temporal information can be obtained. Various tokamak scenarios will be discussed in this paper. Different methods for the mitigation of the impact of Type I ELMs are currently investigated in fusion research. In this paper we will summarize the effect of seeded impurities on the divertor power load and we will present a first analysis of space resolved ELM-measurements obtained from strike point sweeps.

## 1. DISCHARGES WITH IMPURITY SEEDING USING NOBLE GASES

The aim of impurity seeding is the formation of a radiating belt with simultaneous achievement of high densities with good confinement properties as it has been demonstrated on TEXTOR [1]. Impurity seeding has been studied also on JET ELMy H-Modes in the past years. In the discharges studied in this paper, two main phases can be distinguished, the so-called puff-phase with a large puff of D and Ar (to increase the density and the radiation fraction), followed by the afterpuff phase, where only gentle D and Ar puffing is applied to reach a stationary high performance phase. The scenario and its properties have been described in more detail in [2]. In the following we will mainly focus on the afterpuff-phase, due to its good confinement properties. Figure 1 shows a typical example of a JET Argon seeded discharge (red curves) together with a reference pulse without Ar seeding (blue curves). Both pulses have been performed at  $B_t = 2.4$  T,  $I_p = 2.5$  MA, with auxiliary heating at a level of  $P_{in} = 13$  MW. The reference pulse has a slightly higher gas-level during the puff-phase, which results in a higher target density. However this is not of importance for the study presented here. During Argon seeding, a rise is observed in the total radiated power  $P_{rad,tot}$ . Abel-inversion of the bolometer shows that in the puff-phase the additional radiation causes enhanced divertor and X-point radiation, whereas in the afterpuff phase the power radiated in the plasma volume is clearly increased (dashed lines). Therefore the power crossing the separatrix,  $P_{sol} (=P_{in}-P_{rad,core})$  is lowered and hence the ELMs are delayed [3]. As it can be inferred from Fig. 1 the contribution of the radiation in the plasma volume to the total radiation increases from 35% to 50%.

The question is, where the input power goes. Since the plasma is in steady-state during the after-puff,  $dW/dt$  is small.  $P_{in}$  divides therefore solely into radiation losses and heat losses by particles. The divertor tiles will absorb the power radiated in the divertor and the convective heat losses. The total absorbed power is monitored by thermocouples, which are embedded in the tiles. Figure 2 shows the energy, which has been absorbed over the whole pulse by the inner and outer divertor tiles and the

divertor base plates. The largest decrease in the absorbed energy caused by the Argon seeding is seen at the outer vertical divertor tiles. The thermocouple data show a reduction of the absorbed energy at the inner and outer divertor tiles by about 14MJ, which is in good agreement with the reduction of the energy  $E_{\text{sol}}$ , entering the scrape-off layer, from 99MJ to 86MJ ( $=\int(P_{\text{in}}-P_{\text{rad,core}}) dt$ ). Seven megajoule of this decrease are achieved in the afterpuff phase, showing that the Ar seeded in the afterpuff has a significant effect on the energy absorbed by the divertor. The absorbed energy changes by the same percentage at the inner and outer divertor. By comparing  $E_{\text{sol}}$  with  $E_{\text{div}}$ , we find a decrease in the convective heat load onto the divertor by 16MJ ( $=\int(E_{\text{sol}}-E_{\text{div}}) - (E_{\text{sol}} \text{ Ar} - E_{\text{div}} \text{ Ar})$ ) for the Ar-seeded pulse. It is obvious that not only the conductive heat losses are affected by the Argon, but that also the convective heat losses can be reduced. To study the convective heat losses, data from triple Langmuir probe measurements have been analyzed. The result can be seen in Fig.3, where the averaged ELM time traces at the inner and outer divertor each time at two different locations are plotted. The timer traces of heat flux parallel to the magnetic field lines  $Q_p$  have been coherently averaged with respect to the  $D\alpha$ -signal during the afterpuff phase. Note that there is a slight delay between the probe-signal and the  $D\alpha$ -signal. The cause for this delay is at the moment not clear. A technical jitter cannot be excluded. The profiles effects are different for the inner and outer divertor. The ELM-peak at the inner strike zone does not change when Argon is seeded, but the impact zone of the heat on the divertor shrinks, since the measured parallel heat flux  $Q_p$  is smaller at a location away from the strike point. At the outer divertor however, the heat flux at the strike point decreases dramatically, when the ELM arrives, and the total wetted area is broadened. The rise time and decay time of the ELM seem not to be significantly affected by the Argon. The particle fluxes at the outer strike zone decrease by a much smaller amount than  $Q_p$ , which suggest that drop in  $Q_p$  is due to a lower temperature of the arriving particles. It appears interesting to note that Ar seeding has almost no effect on the profile in between ELMs, besides a slight increase of the electron temperature and heat flux at the inner divertor. Due to the lack of available probes the total heat and particle fluxes towards the divertor tiles could not be determined. However an attempt has been made to measure those in discharges optimised for diagnostic measurements, and are presented in the following section.

### 3. SPACE- AND TIME- RESOLVED ELM-MEASUREMENTS

Assuming a regular and similar arrival of ELMs at the divertor targets, induced strike point sweeps and voltage ramps can be used to reconstruct either deposition profiles of heat and particles or to improve the probe measurements by applying the single probe technique, where the full I(V)-characteristic is determined. Figure 4 shows an exemplary discharge in the so-called diagnostic optimized configuration (DOC) at low triangularity  $\delta = 0.25$  with Type-I ELMs ( $P_{\text{NBI}} = 13\text{MW}$ ,  $q_{95} = 3.8$ , Greenwald-fraction  $f_{\text{gw}} = 0.75$ ) used for two different probe settings. In one case (red curves in 4th and 5th box) the inner and outer strike point have been moved down by 5cm and 8cm respectively during the steady state phase between 19 and 23sec. For this pulse the applied probe voltage has been

kept constant at  $V_{pr} = -100\text{V}$  to measure the particle flux (see box 6 of Fig.4). The ELM behaviour is nearly unchanged, when the strike points are moved. Using the  $D_\alpha$ -signal as a marker, the saturation current of a probe has been sorted in time with respect to its relative position to the strike point (see ref. [4]). The result can be seen in Fig.5, where the particle flux is displayed as a function of time and radius. The quantity  $d_{sep}$  is the vertical distance of the probe to the strike point, with negative values corresponding to the private flux region. The value  $d_{sep} = 0$  corresponds to the strike point position as obtained from equilibrium reconstruction. The inaccuracy of the EFIT evaluation causes a displacement of the strike point position. Contrary to what one would expect, the radial decay of the particle flux is not as steep as in L-mode discharges. The level of the probe voltage has been changed in consecutive pulses to obtain several points in the I(V) curve to determine the electron temperature. The disadvantage of such approach (similar to the triple probe set-up) however is that it assumes the energy distribution of the electrons to be Maxwellian and an exponential decay of the current is inhibited. In another case the strike points have been adjusted at a fixed position (see blue curves in boxes (d) and (e)). The probe voltage has then slowly ramped to allow the reconstruction of the I(V)-characteristica during all ELM-times. A first analysis has shown a fair agreement of electron temperature derived from the two different methods.

## CONCLUSIONS.

Globally, the heat load on the divertor caused by ELMs can be reduced by Argon-seeding. However locally unfavorable effects arise: the heat flux profile at the inner divertor shrinks, keeping the heat flux at the strike zone about the same. Particle flux is much more decreased, than  $Q_p$ , which indicates a higher temperature of the arriving particles. At the outer divertor seeding of Argon reduces the heat flux over the full deposition profile, but one has to be aware of the limited spatial resolution. It was possible to reconstruct the ELM-deposition profile by coherent averaging of pulses, which had strike point sweeps. It has been found that the profile of the particle flux is broad during the ELM-peak and that it extends far into the private flux region. Further analysis and comparison with Infrared-measurements are under way.

## REFERENCES

- [1]. A. Messiaen et al, Phys. Rev. Letters **77** (1996), p. 2487.
- [2]. P. Dumortier et al, Plasm. Phys. Contr. Fus. **44** (2002), p 1845.
- [3]. S. Jachmich et al, Plasm. Phys. Contr. Fus. **44** (2002), p. 1879.
- [4]. M. Laux et al, 28 th EPS-Conference, Madeira, Portugal (2001), P4.081.

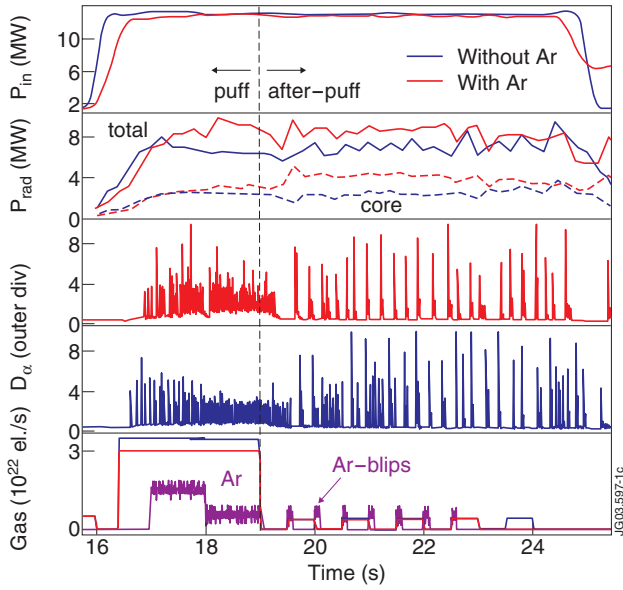


Figure 1: JET ELMy H-mode discharges (Pulse No.:s 52161, 53031) with (red traces) and without (blue traces) Argon-seeding. The time traces are (from top to bottom) total input power (12.5MW NBI), total (solid) and core (dashed) radiation, recycling at the outer divertor, gas rates of  $D_2$  and Ar (only in red discharge).

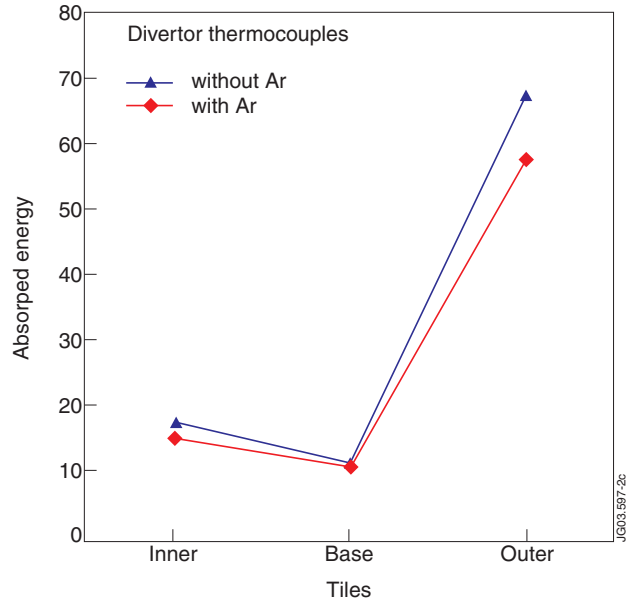


Figure 2: Energy absorbed in the divertor by the two inner tiles, two base tiles incl. septum and the two outer tiles.

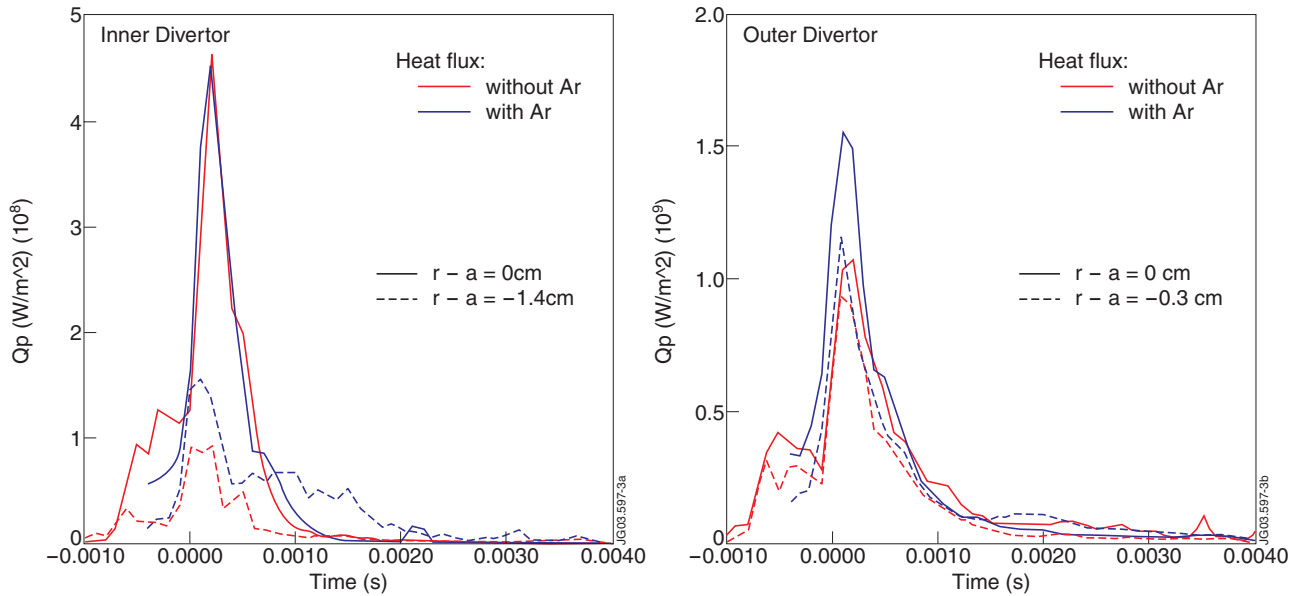


Figure 3: Heat flux to inner and outer divertor, measured by triple probes. The data are averaged over the afterpuff-phase from 20 to 23 sec. The value  $r-a$  indicates the probe position with respect to the separatrix, mapped onto the midplane



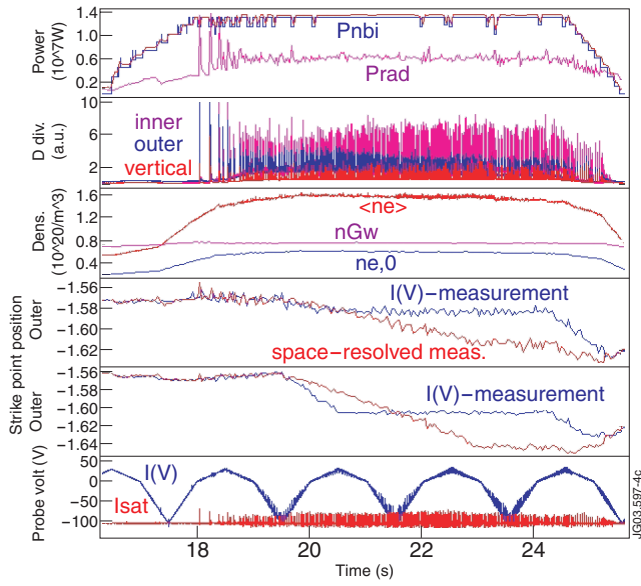


Figure 4: JET Type-I ELMy H-mode discharges (Pulse No: 58574, 58632) with two different settings.

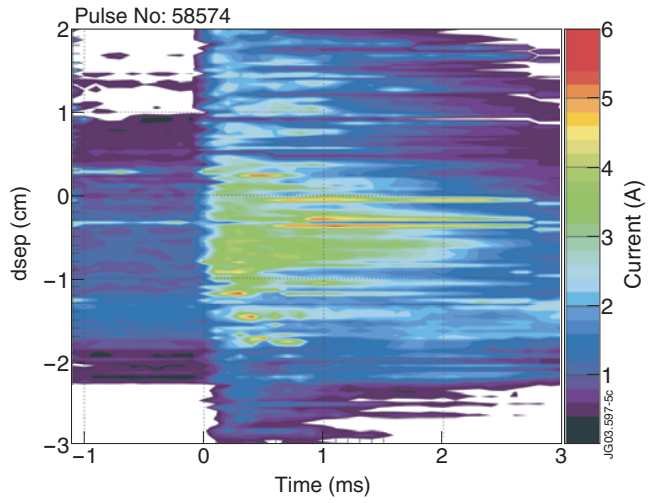


Figure 5: Contour plot of saturation current measured at the outer divertor during strike point sweeps after coherent averaging.